Journal Name

RSCPublishing

COMMUNICATION

Distance measurements between manganese(II) and nitroxide spin-labels by DEER determine a binding site of Mn^{2+} in the HP92 loop of ribosomal RNA

Cite this: DOI: 10.1039/xoxxoooooox

Received ooth January 2012,
Accepted ooth January 2012

DOI: 10.1039/xoxxoooooox

www.rsc.org/

Ilia Kaminker[a] , Morgan Bye[a], Natanel Mendelman[a], Kristmann Gislason[a], Snorri Th. Sigurdsson[b] and Daniella Goldfarb[b,*]

Mn^{2+} localization in hairpin 92 of the 23S ribosomal RNA (HP92) was obtained using high field, W-band (95 GHz), DEER (double electron-electron resonance) distance measurements between the Mn^{2+} and nitroxide spin labels on the RNA. It was found to be preferably situated in the minor groove of the double strand region close to the HP92 loop.

The DEER (double electron-electron resonance) technique[2, 3] has become very popular in recent years for obtaining nanometer scale distance restrains in structural studies of biomolecules in frozen solutions.[4-7] The most common application of DEER is to measure distances between two nitroxide spin labels attached at specific points of interest in a biomolecule. It has also been successfully applied to determine the distances between other types of paramagnetic centers in biomolecules[8], such as Cu^{2+}-Cu^{2+} [9, 10], Gd^{3+}-Gd^{3+} [11-13], Mn^{2+}-Mn^{2+} [14], pairs of iron-sulfur clusters[15, 16] and trityl-trityl radicals[17, 18]. Biomolecular hetero-spin label distance measurements, including nitroxide -Cu^{2+} [19-21] nitroxide - iron-sulfur cluster[22] and nitroxide - Gd^{3+} [23, 24], have also been reported. A recent important alternative application of DEER, in combination with site directed spin labelling, has been locating metal ion binding sites by means of paramagnetic metal ion - nitroxide distance measurements in a biomolecule, as has been demonstrated in on Cu^{2+} binding sites. [21,19]

Metal ions play a crucial role in RNA structure and function.[25] They stabilize its tertiary structure[25-31] and are essential for catalysis in ribozymes.[31] Several types of RNA-metal ion interactions, that can take place simultaneously, are recognized. One type involves poorly localized "diffuse ions", the charge of which balance the negative charge of the phosphodiester backbone of the RNA.[32] The second type involves ions with specific interactions at particular sites on the RNA molecule.[32] These bind either through inner-sphere interactions involving direct coordination to the electronegative RNA functional groups, or via outer-sphere interactions mediated by water ligands.[31] K^+ and Mg^{2+} ions are usually considered the natural metal ion cofactors for nucleic acids *in vivo*. Mg^{2+}, however, presents a challenge for optical and magnetic spectroscopic characterization. One way of overcoming this limitation is to substitute it with the paramagnetic Mn^{2+} ion, which has a similar radius and charge,[33] and apply EPR spectroscopic methods.[34, 35] High resolution EPR methods that are typically used to probe Mn^{2+} binding sites in RNA yield local information, such as the hyperfine coupling with ^{14}N from the nucleobases and phosphate ^{31}P. While providing important structural information on the nature of the metal ion ligation, these methods, however, do not give direct information on the location of the binding site within the RNA.

In this communication we introduce high field (W-band, 95 GHz) Mn^{2+}-nitroxide DEER distance measurements for locating Mn^{2+} binding sites in RNA. We demonstrate this approach by locating a Mn^{2+} binding site in an RNA derived from hairpin 92 of the 23S ribosomal RNA (HP92). HP92 is a specific target to DbpA and YxiN RNA helicases (from *Escherichia coli* and *Bacillus subtilis* respectively). The feasibility of Mn^{2+}-nitroxide DEER measurements has been recently reported on a rigid model compound.[36]

Figure 1a shows the RNA construct used in this study and the spin labelling positions. Three HP92 RNA constructs were prepared: two singly labelled, (RNA(3) and RNA(31)), and one doubly labelled RNA (RNA(3,31). Several methods exist for site-directed spin labelling (SDSL) of nucleic acids,[37] but we chose post-synthetic labelling of 2′-amino groups with 4-

isocyanto-TEMPO (Fig. 1b).[38] (see supplementary information (SI) for details).

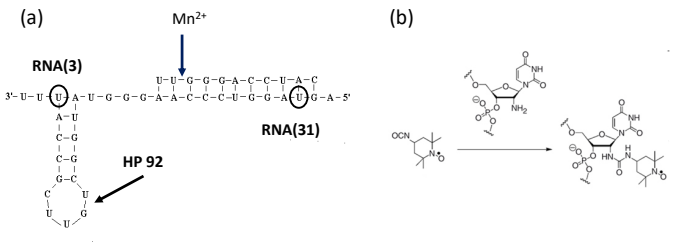

Figure 1. (a) The sequence and the secondary structure of the RNA construct studied. The spin labelling positions are indicated with circles. The putative location of the Mn^{2+} as determined by the DEER measurements is indicated by an arrow. (b) The RNA spin-labelling scheme.

Measurements were carried out at W-band because of the high sensitivity that it features for Mn^{2+}, which is a half integer, high spin ion (S=5/2). This arises from the reduced inhomogeneous broadening of the $|-1/2> \rightarrow |1/2>$ transition by the zero field splitting (ZFS) at high fields.[39] First, DEER measurements were carried out on the doubly labelled RNA(3,31), without the addition Mn^{2+} or Mg^{2+}, to obtain structural restrains on the RNA itself and results are shown in Fig. 2. Measurements were carried out at three observer magnetic field positions to check for orientation selection[40] (see Fig. S1, and SI for experimental details). All three measurements gave a similarly broad distance distribution, spanning a width of ~ 3 nm with a maximum in the range of 4.5- 4.9 nm. In light of the width of the distribution and the lowest signal to noise ratio (SNR) of the "g_{zz}" trace, which gave the 4.5 nm maxima, we consider this range to be within experimental error and ignore orientation selection. The broad distance distribution is attributed to the nitroxide label local flexibility and high flexibility of the RNA. This is consistent with the room temperature X-band CW-EPR spectra (Fig. S1) of RNA(3) and RNA(31) that are typical of nitroxides attached to highly flexible biomolecule.

Mn^{2+} - nitroxide (Mn-NO) DEER measurements on Mn^{2+}/RNA(3) and Mn^{2+}/RNA(31) complexes (1:1 Mn^{2+}:RNA molar ratios) are shown in Fig. 3. Here the different spectroscopic properties of Mn^{2+} and the nitroxide spin label have to be carefully considered when the experiment is set up. EPR spectra of these samples and additional experimental details are presented in the SI.

In the Mn-NO DEER measurements, the observer pulses were set to the 3rd hyperfine line of the Mn^{2+} sextet, the pump pulse was set to either the maximum ($\Delta\nu$ = -120MHz) or more towards the g_{zz} position ($\Delta\nu$ =-65MHz) of the nitroxide spectrum (Fig. S2c). By observing the Mn^{2+} signal we take advantage of its fast spin lattice relaxation rate that allows for fast signal averaging. This set up also minimizes the contribution of the nitroxide to the observed signal because of its saturation. In addition, the narrower nitroxide spectrum allows a higher modulation depth, namely more spins are affected by the pump pulse. [23] Figures 3a,b present the DEER data of Mn^{2+}/RNA(31) and the distance distribution obtained after fitting to a two Gaussians model. These measurements gave distance distribution with a narrow Gaussian at 2.3-2.4 nm superimposed on a much broader one with a width around 3.0 nm and a maximum at 2.5 nm. The data could not be satisfactory fitted with one Gaussian. Data analysis using

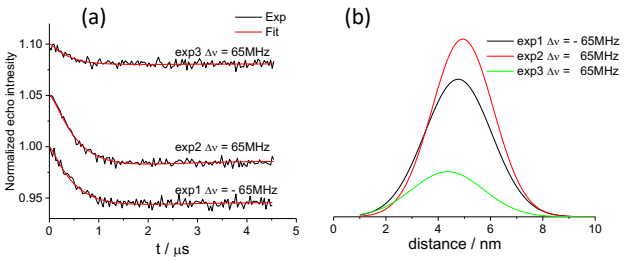

Figure 2. (a) DEER traces measured on RNA(3,31) after background removal along with the fit (red trace) obtained with the distance distribution shown in (b). The two upper DEER traces in (a) were shifted for clarity. Raw DEER data is presented in Figure S3a; Data analysis was performed with DeerAnalysis.[1] Sample composition was 166 µM RNA / 33 mM HEPES / 66 mM NaCl / 33% d3-glycerol in D_2O

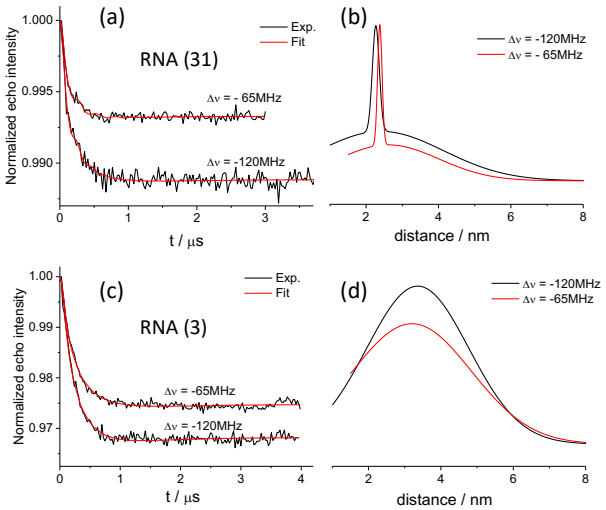

Figure 3. DEER traces of Mn^{2+}/ RNA(31) (a) and Mn^{2+}/ RNA(3) (b) obtained for two Δν values after background removal along with the fit (red trace) derived with the distance distribution shown in (c) and (d) respectively. The raw DEER traces are given in Fig. S3b,c. All DEER measurements were carried out at 10K and repetition time of 1 ms. Data analysis was done with DeerAnalysis.[1] Sample compositions were 135 µM RNA / 135µM $MnCl_2$, 31mM HEPES / 62mM NaCl, 41% d3-glycerol in D_2O

Tikhonov regularization gave results consistent with this interpretation. (See Fig. S4 and discussion in the SI for details). DEER data of Mn^{2+}/ RNA(3) are shown in Fig. 3c. Here the DEER traces could be satisfactorily fitted with a single Gaussian, with a broad distribution and a maximum at 3.6 nm (Fig 3d). In neither constructs did we observe orientation selection as reported for W-band Gd^{3+}-nitroxide DEER measurements.[40] In combining the NO-NO distances obtained from RNA(3,31) with those obtained from the Mn-NO results we assumed that addition of the equimolar amount of Mn^{2+} did not alter the structure of the RNA significantly.

W-band ENDOR (electron-nuclear double resonance) measurements of Mn^{2+} with non- labeled RNA revealed no ^{31}P hyperfine couplings. This is unlike the single strand HP92, without the 11 base complementary strand, which showed a clear ^{31}P coupling of ~9 MHz, typical of Mn^{2+} bound to phosphate of the backbone.[41] In addition, X-band electron spin echo envelope modulation (ESEEM) measurements did not reveal any coupling to ^{14}N, excluding the presence of a direct binding to an ^{14}N of a nucleobase, a binding mode similar to one observed in the Hammerhead ribozyme with direct coordination to N7 nitrogen atoms of adenine and guanine.[42-44] These findings suggest that the Mn^{2+} ion is bound to HP92 through an outer-sphere coordination. This mode of binding is similar to that reported for type 0 coordination of Mg^{2+} in the crystal structure of the large ribosomal subunit, which features hydrogen bonds involving six water molecules and zero direct contacts with RNA hydrophilic atoms.[45, 46]

The DEER results show that Mn^{2+} does bind to the HP92 constructs studied, although no ^{14}N or ^{31}P ENDOR signals were observed. The observed broad distance distribution could be due to either non-specific Mn^{2+} binding-sites on the RNA construct or flexibility of the RNA construct and/or the spin label. Both the X-band CW EPR spectrum of RNA(3) (Fig. S1) and the broad nitroxide-to-nitroxide distance distribution obtained for

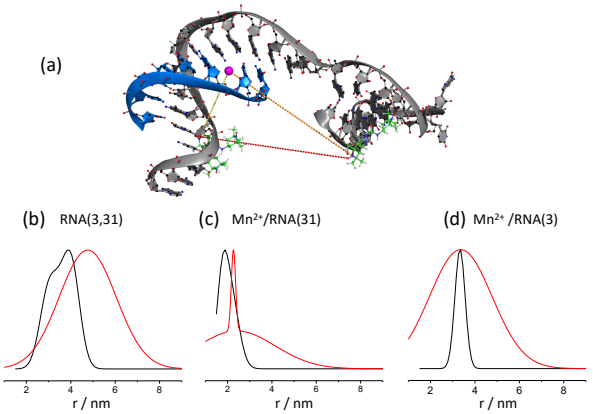

RNA(3,31) (Fig. 2) indicate substantial flexibility of the label. On the other hand, the fact that we observe a superposition of a narrow and a broad distance distribution for Mn^{2+}/RNA(31) indicates that the presence of non-specific sites cannot be excluded. The distance of 2.3-2.4 nm observed for RNA(31) suggests the presence of a specific Mn^{2+} binding site somewhere in the double stranded region of the 5' extension of the RNA construct. This is supported by the observed change in the coordination sphere of Mn^{2+} in HP92 upon binding of the 11-base complementary strand.[41] Furthermore, the observation of a narrow distance distribution, that was distinct from the broad background, for RNA(31) construct, but not for RNA(3) construct, suggests that the broadening in the latter has significant contributions from the flexibility in the linker region between HP92 and the double stranded region of the 5' extension of the RNA construct.

The modulation depth observed, with the pump pulse set to the maximum of the nitroxide spectrum, was 1.2 % for Mn^{2+}/RNA(31) and ~3.0 % for Mn^{2+}/RNA(3). This is significantly lower than the ~5.5 % observed for the nitroxide-nitroxide distance measurements, indicating that the binding affinity of the Mn^{2+} is not high and that there are free "diffuse" Mn^{2+} ions in solution. Measurements on a nitroxide-nitroxide model compound, under the same pump pulse parameters gave ~10 % modulation depth, suggesting that the labeling efficiency was not 100%.[47, 48] Thus, the difference in modulation depth between the two constructs is attributed to differences in labeling efficiencies.

To substantiate the localization of the Mn^{2+} in the region of the 5' extension of the RNA construct we used a simple-minded model, taking the X-ray crystallography-derived RNA binding domain of YxiN bound to an extended fragment (nucleotides 2508-2580) of the 23S ribosome from *E. coli* (PDB: 3MOJ) as a template for the structure of the HP92[49, 50] and added to it the spin labels using MtsslWizard[51] (details are given in the SI).

Calculated DEER distance distributions were adapted from MtsslWizard's Distance mode taking into account all possible rotamers of the spin label, while keeping the RNA rigid.[51] Figure 4a highlights the spin label rotamers, yielding the shortest and longest distances to the Mn^{2+} position. In the case of the spin label on 31, two distinct rotamer clouds were possible due to the curvature of the backbone, one internalized to the helix with a narrow distance distribution and a second broader cloud on the exterior of the helix curvature. Accordingly, Fig. 4a shows three rotamers at this position, two corresponding to the first cloud's shortest and longest distances and the third that corresponds to the second cloud's average. The distance for RNA(3,31), shown in Fig. 4b, yields a distance distribution with a maximum at 4.0 nm, which is shorter than the experimental result, ~4.9 nm. This suggests that in solution the structure of HP92 is on the average more extended. Moreover, the calculated distance distribution is significantly narrower than the experimentally derived distance distribution, which implies a large conformational flexibility of the HP92 construct in solution.

Figure 4. (a) The HP92 (grey)+ 11 base complementary strand model (blue) and the Mn^{2+} (pink) location . Some of the nitroxide spin label rotamers are shown in green . Left are three rotamers in the 31 position, while on the right there are two rotamers in the 3 position. The lines highlight some nitroxide-nitroxide and Mn^{2+}-nitroxide distances. (b-d) The calculated distance distributions for the various constructs using this model (black) compared with the experimental ones (red).

While placing the Mn^{2+}, it was taken as a hexaaqua complex, approximated as a sphere of diameter 1.0 nm (metal diameter + 2x bond length + 2x water's Van der Waals radius), with assumed position minimizing distortion of nucleotide bases and minimizing energy. It was placed in a position that would give the best agreement with the DEER data. According to this model, the Mn^{2+} is placed in a minor grove in the RNA twist shown in Fig. 4a (pink sphere). This position is also indicated as an arrow in Fig. 1a, to highlight the specific bases in the vicinity. Interestingly, outersphere hydrated Mg^{2+} ions are often found in the deep groove of A-form helices, forming hydrogen bonds to acceptors atoms of the guanine base.[46] This yields a most probable Mn^{2+} -nitroxide distance Mn^{2+}/RNA(31) around 1.9 nm (Fig. 4c), which is rather close to the observed 2.3-2.4 nm. The modeled Mn^{2+}/RNA(3) distance is 3.3 nm (Fig. 4d), also close to the experimentally observed distance of 3.6 nm. A reduced RNA backbone curvature, as suggested by the experimentally derived RNA(3,31) distance distribution, would generate a longer distance between the Mn^{2+} and nitroxide spin labels and a better agreement. While this simplistic modelling suggest a reasonable location for the Mn^{2+} ion, in the future systematic molecular dynamics simulations should be carried out on the RNA, including the solvent and the Mn^{2+} ion to obtain the energy landscape of the Mn^{2+} potential coordination site and account for the multiple RNA conformation in solution, taking into account the experimentally derived distance distributions.

Conclusions

We have demonstrated that Mn^{2+}-nitroxide W-band DEER distance measurements can be added to the tool-box used for localizing Mn^{2+} binding-sites in nucleic acids, particularly when the Mn^{2+} (or Mg^{2+}) play a role in structure stabilization or catalysis. Our results show that HP92 with its 11 base complementary strand in solution is extended relative to the crystal structure and highly flexible. We identified a specific binding site for outer-sphere coordinated Mn^{2+} in the minor groove of the double stand region close to the HP92 loop. In the future, the use of rigid spin labels[52] would yield data where any observed flexibility could be directly traced to movements of the RNA, eliminating contributions from the spin label tether and will potentially allow for more precise localization of the binding sites.

ACKNOWLEDGMENT

We thank Anastasiya Sushenko for her tremendous help in sample preparation. This work was supported by the Minerva foundation with funding from the Federal German Ministry for Education and Research and in part made possible by the historic generosity of the Harold Perlman Family. D.G holds the Erich Klieger Professorial Chair in Chemical Physics.

REFERENCES

1. G. Jeschke, V. Chechik, P. Ionita, A. Godt, H. Zimmermann, J. Banham, C. R. Timmel, D. Hilger and H. Jung, *Appl. Magn. Reson.*, 2006, **30**, 473-498.
2. A. D. Milov, A. B. Ponomarev and Y. D. Tsvetkov, *Chem. Phys. Lett.*, 1984, **110**, 67-72.
3. M. Pannier, S. Veit, A. Godt, G. Jeschke and H. W. Spiess, *J. Magn. Reson.* 2000, **142**, 331-340.
4. P. Borbat and J. Freed, in *Structural Information from Spin-Labels and Intrinsic Paramagnetic Centres in the Biosciences*, eds. C. R. Timmel and J. R. Harmer, Springer Berlin Heidelberg, 2013, vol. 152, pp. 1-82.
5. G. Jeschke, in *Structural Information from Spin-Labels and Intrinsic Paramagnetic Centres in the Biosciences*, eds. C. R. Timmel and J. R. Harmer, Springer Berlin Heidelberg, 2013, vol. 152, pp. 83-120.
6. R. Ward and O. Schiemann, in *Structural Information from Spin-Labels and Intrinsic Paramagnetic Centres in the Biosciences*, eds. C. R. Timmel and J. R. Harmer, Springer Berlin Heidelberg, 2013, vol. 152, , pp. 249-281.
7. W. L. Hubbell, C. J. Lopez, C. Altenbach and Z. Yang, *Curr. Opin. Struct. Biol.* , 2013, **23**, 725-733.
8. D. Goldfarb, in *Structural Information from Spin-Labels and Intrinsic Paramagnetic Centres in the Biosciences*, eds. C. R. Timmel and J. R. Harmer, Springer Berlin Heidelberg, 2013, vol. 152, pp. 163-204.
9. I. M. C. van Amsterdam, M. Ubbink, G. W. Canters and M. Huber, *Ange. Chem. Int. Ed.* 2003, **42**, 62-64.
10. C. W. M. Kay, H. El Mkami, R. Cammack and R. W. Evans, *J. Am. Chem. Soc.*, 2007, **129**, 4868-4869.
11. A. Potapov, H. Yagi, T. Huber, S. Jergic, N. E. Dixon, G. Otting and D. Goldfarb, *J. Am. Chem. Soc.* 2010, **132**, 9040-9048.
12. H. Yagi, D. Banerjee, B. Graham, T. Huber, D. Goldfarb and O. Gottfried, *J. Am. Chem. Soc.*, 2011, **133,**, 10418-10421
13. Devin T. Edwards, T. Huber, S. Hussain, Katherine M. Stone, M. Kinnebrew, I. Kaminker, E. Matalon, Mark S. Sherwin, D. Goldfarb and S. Han, *Structure*, 2014, **22**, 1677-1686.
14. D. Banerjee, H. Yagi, T. Huber, G. Otting and D. Goldfarb, *J. Chem. Phys. Lett.*, 2012, **3**, 157-160.
15. C. Elsasser, M. Brecht and R. Bittl, *J. Am. Chem. Soc.*, 2002, **124**, 12606-12611.
16. P. P. Borbat and J. H. Freed, *Chem. Phys. Lett.*, 1999, **313**, 145-154.
17. Z. Yang, Y. Liu, P. Borbat, J. L. Zweier, J. H. Freed and W. L. Hubbell, *J J. Am. Chem. Soc.*, 2012, **134**, 9950-9952.
18. G. Y. Shevelev, O. A. Krumkacheva, A. A. Lomzov, A. A. Kuzhelev, O. Y. Rogozhnikova, D. V. Trukhin, T. I. Troitskaya, V. M. Tormyshev, M. V. Fedin, D. V. Pyshnyi and E. G. Bagryanskaya, *J. Am. Chem. Soc.* 2014, **136**, 9874-9877.

19. D. Abdullin, N. Florin, G. Hagelueken and O. Schiemann, *Angew. Chem. Int. Ed.* 2015, **54**, 1827-1831.
20. G. E. Merz, P. P. Borbat, A. J. Pratt, E. D. Getzoff, J. H. Freed and B. R. Crane, *Biophy. J.* , 2014, **107**, 1669-1674.
21. Z. Yang, M. R. Kurpiewski, M. Ji, J. E. Townsend, P. Mehta, L. Jen-Jacobson and S. Saxena, *Proc. Nat. Acad. Sci. USA*, 2012, **109**, E993-E1000.
22. J. E. Lovett, A. M. Bowen, C. R. Timmel, M. W. Jones, J. R. Dilworth, D. Caprotti, S. G. Bell, L. L. Wong and J. Harmer, *Phys. Chem. Chem. Phys.*, 2009, **11**, 6840-6848.
23. I. Kaminker, H. Yagi, T. Huber, A. Feintuch, G. Otting and D. Goldfarb, *Phys. Chem. Chem. Phys.*, 2012, **14**, 4355-4358.
24. L. Garbuio, E. Bordignon, E. K. Brooks, W. L. Hubbell, G. Jeschke and M. Yulikov, *J. Phys. Chem. B*, 2013, **117**, 3145-3153.
25. A. Sigel, H. Sigel and R. K. O. Sigel, eds., *Structural and Catalytic Roles of Metal Ions in RNA,* Royal Society of Chemistry, Cambridge, UK, 2011, Vol 9.
26. A. M. Pyle, *J. Biol. Inorg. Chem.*, 2002, **7**, 679-690.
27. S. A. Woodson, *Curr. Opin. Chem. Biol.*, 2005, **9**, 104-109.
28. T. A. Steitz and J. A. Steitz, *Proc. Nat. Acad. Sci. USA*, 1993, **90**, 6498-6502.
29. V. J. DeRose, *Curr. Opin. Struct. Biol.* , 2003, **13**, 317-324.
30. A. R. Ferre-D'Amare and W. C. Winkler, in *Structural and Catalytic Roles of Metal Ions in RNA*, The Royal Society of Chemistry, 2011, vol. 9, pp. 141-173.
31. A. E. Johnson-Buck, S. E. McDowell and N. G. Walter, in *Structural and Catalytic Roles of Metal Ions in RNA*, The Royal Society of Chemistry, 2011, vol. 9, pp. 175-196.
32. Z.-J. Tan and S.-J. Chen, in *Structural and Catalytic Roles of Metal Ions in RNA*, The Royal Society of Chemistry, 2011, vol. 9, pp. 101-124.
33. G. H. Reed and R. R. Poyner, *Metal Ions in Biological Systems*, 2000, **37**, 183-207.
34. M. C. Erat and R. K. O. Sigel, in *Structural and Catalytic Roles of Metal Ions in RNA*, The Royal Society of Chemistry, 2011, vol. 9, pp. 37-100.
35. L. Hunsicker-Wang, M. Vogt and V. J. DeRose, in *Methods in Enzymology, Vol 468: Biophysical, Chemical, and Functional Probes of RNA Structure, Interactions and Folding, Pt A*, ed. D. Herschalag, 2009, vol. 468, pp. 335-367.
36. D. Akhmetzyanov, J. Plackmeyer, B. Endeward, V. P. Denysenkov and T. F. Prisner, *Phys. Chem. Chem. Phys.* 2015, **14**, 6760-6766
37. S. A. Shelke and S. T. Sigurdsson, *Eur. J. Org. Chem*, 2012, **12**, 2291-2301.
38. T. E. Edwards, T. M. Okonogi, B. H. Robinson and S. T. Sigurdsson, *J. Am. Chem. Soc.*, 2001, **123**, 1527-1528.
39. P. Manikandan, R. Carmieli, T. Shane, A. J. Kalb and D. Goldfarb, *J. Am. Chem. Soc.*, 2000, **122**, 3488-3494.
40. I. Kaminker, I. Tkach, N. Manukovsky, T. Huber, H. Yagi, G. Otting, M. Bennati and D. Goldfarb, *Embo J.*, 2001, **20**, 4214-4221. 2013, **227**, 66-71.
41. I. Kaminker, A. Sushenko, A. Potapov, S. Daube, B. Akabayov, I. Sagi and D. Goldfarb, *J. Am. Chem. Soc.*, 2011, **133**, 15514-15523.
42. S. R. Morrissey, T. E. Horton, C. V. Grant, C. G. Hoogstraten, R. D. Britt and V. J. DeRose, *J. Am. Chem. Soc.*, 1999, **121**, 9215-9218.
43. M. Vogt, S. Lahiri, C. G. Hoogstraten, R. D. Britt and V. J. DeRose, *J. Am. Chem. Soc.*, 2006, **128**, 16764-16770.
44. O. Schiemann, J. Fritscher, N. Kisseleva, S. T. Sigurdsson and T. F. Prisner, *Chembiochem*, 2003, **4**, 1057-1065.
45. D. J. Klein, T. M. Schmeing, P. B. Moore and T. A. Steitz, *Embo J.*, 2001, **20**, 4214-4221.
46. P. Auffinger, N. Grover and E. Westhof, in *Structural and Catalytic Roles of Metal Ions in RNA*, The Royal Society of Chemistry, 2011, vol. 9, pp. 1-36.
47. F. Mentink-Vigier, A. Collauto, A. Feintuch, I. Kaminker, V. T. Le and D. Goldfarb, *J. Magn. Reson.*, 2013, **236**, 117-125.
48. I. Kaminker, M. Florent, B. Epel and D. Goldfarb, *J. Magn. Reson.*, 2011, **208**, 95-102.
49. J. W. Hardin, Y. X. Hu and D. B. McKay, *J. Mol. Biol.*, 2010, **402**, 412-427.
50. S. Y. Wang, Y. X. Hu, M. T. Overgaard, F. V. Karginov, O. C. Uhlenbeck and D. B. McKay, *RNA,* 2006, **12**, 959-967.
51. G. Hagelueken, R. Ward, J. H. Naismith and O. Schiemann, *Appl. Magn. Reson.*, 2012, **42**.
52. N. Barhate, P. Cekan, A. P. Massey and S. T. Sigurdsson, *Angew. Chemi. Intel. Ed.*, 2007, **46**, 2655-2658.

Notes and references

[a] Department of Chemical Physics, Weizmann Institute of Science, Rehovot 76100, Israel.

[b] University of Iceland, Department of Chemistry, Science Institute Dunhaga 3, 107 Reykjavik, Iceland.

.

Electronic Supplementary Information (ESI) available: Sample preparation, X-band EPR spectra, W-band nitroxide – nitroxide DEER details of DEER experimental conditions, Mn^{2+}/nitroxide EDEPR spectra and DEER experimental details, DEER raw data, DEER data analysis using Tikhonov regularization.

See DOI: 10.1039/c000000x/